Results in Nonlinear Analysis 8 (2025) No. 3, 190–199
https://doi.org/10.31838/rna/2025.08.03.015
Available online at www.nonlinear-analysis.com

Results in Nonlinear Analysis
ISSN 2636-7556

Peer Reviewed Scientific Journal

Deep learning and nonlinear optimization-assisted PDE segmentation framework for accurate brain tumor boundary detection in MRI scans

Muruganantham S.[a], Marakhimov Avazjon Rakhimovich[b], Nafisa Abdullayeva[c], Odilbek Kosimov[d], Annette Nellyet[e], C. Arunkumar Madhuvappan[f], S. Valarmathy[g]

[a]Department of Computer Technology and Information Technology, Kongu Arts and Science College (Autonomous), Erode, Tamil Nadu, India; [b]Department of Information Processing and Management Systems, Tashkent State Technical University, Tashkent; [c]Department of Primary Education, Andijan State Pedagogical Institute, Andijan, Uzbekistan; [d]Department of Information Technology and Exact Sciences, Termez University of Economics and Service, Termez, Uzbekistan; [e]University of Stirling, United Kingdom; [f]Department of Biomedical Engineering, Vinayaka Mission's Kirupananda Variyar Engineering College, Salem(Vinayaka Missions Research Foundation), Tamil Nadu, India; [g]Department of Electronics and Communication Engineering, Vinayaka Mission's Kirupananda Variyar Engineering College, Salem, Tamil Nadu, India

Abstract

The correct outline of the brain tumour in magnetic resonance imaging (MRI) is an essential process in the neurosurgical planning process, radiation therapy, and longitudinal monitoring. The framework suggested in this paper combines deep learning with nonlinear partial differential equation (PDE)–based optimization in high-precision tumour boundary segmentation of multi-modal MRI scans. A convolutional neural network (CNN) is initially trained to give an initial approximate tumour and neighboring edema tissues segmentation mask. Second, a level-set module is a PDE-based level-set module, which is driven by nonlinear energy minimization, to refine the boundary, hence imposing smoothness and retaining fine structural information. The optimization parameters are adjusted in an adaptive manner by a deep reinforcement learning optimizer to learn control policies of the PDE energy weights to allow capturing patient-specific variability. Extensive trial on publicly accessible multi-modal MRI brain tumor datasets reveal that the framework proposed achieves significant

Email addresses: muruganandham.s@gmail.com (Muruganantham S); r.maraximov@gmail.com (Marakhimov Avazjon Rakhimovich); na.abdullayeva@mail.ru (Nafisa Abdullayeva); odilbek_qosimov@tues.uz (Odilbek Kosimov); annette.n@stir.ae (Annette Nellyet); arunkumarmadhuvappan@vmkvec.edu.in (C.Arunkumar Madhuvappan); valarmathy@vmkvec.edu.in (S. Valarmathy)

Received October 15, 2025; Accepted November 17, 2025; Online December 29, 2025

enhancement in Dice similarity coefficient (DSC) increase of 4.7 percent as well as decreased 95th-percentile Hausdorff distance (HD95) relative to state-of-the-art deep-learning segmentation on its own. Corrupted input and missing modality robustness tests demonstrate little performance drop (DSC decline less than 1.8 percent). This shows that the combination of deep learning and nonlinear optimization can be used to successfully present accurate and clinically reliable brain tumour boundary detection.

Mathematics Subject Classification (2020): 68T07, 92C55

Key words and phrases: brain tumor segmentation, deep learning, nonlinear optimization, level-set PDE, MRI, boundary delineation

1. Introduction

The brain tumours are still one of the most difficult to examine in neuro-oncology because of their heterogeneous appearance, diffuse borders, and location relative to the critical areas of the brain. Proper definition of the volume of the tumour in MRI images is required in planning treatment, surgeries, radiation and longitudinal monitoring. Although a variety of MRI modalities, such as T1, T1-contrast, T2, and FLAIR exist, the segmentation task has a significant computational complexity due to the multimodal fusion, which increases the data dimensionality as well as variability [6],[7] [8],[11]. Manual annotation remains the gold standard in clinical practises, however, it is slow, laborious and likely to be inter-observer variable particularly in tumour subregions which are difficult to sub-define like enhancing cores, necrotic tissue and infiltrative edoema [1], [4],[5].

Deep learning has emerged as the method to perform brain tumour segmentation dominating the classical machine-learning and hand-crafted feature-based methods with major improvements. Encoder-decoder architectures, attention-based models, and hybrid CNN-transformer designs have good representational ability, but still fail in incomplete tissue contrast, low-resolution boundary regions, irregular tumour morphology, and missing modalities cases [3], [14], [15]. These models tend to produce a rough prediction with blurred tumour interfaces, which restricts the reliability of such models in clinical use where accuracy under one millimeter is needed around eloquent areas of the cortex [10],[16],[17]. Despite the fact that multimodal fusion and attention processes have mini-mized ambiguities, the accuracy of boundaries is still not suitable to be incorporated in neurosurgical procedures.

In order to supplement data-driven models, a variety of methods rely on classical principles of image-analysis, e.g. active contours, level-set evolution, or variational PDEs. These techniques impose smoothness, regularity of curvature and shape priors that do not emerge naturally in deep learning [9], [18]. Nonetheless, PDE-based segmentation is sensitive to parameters and a set of fixed weights cannot generalize to different patients with varying tumour phenotypes. The traditional PDE models have been hampered by parameter sensitivity, slow convergence, and a low level of flexibility; thus, they do not reach a level of usage in automated pipelines [19]. There is recent evidence that coarse DL output can be used in combination with PDE-based refinement to achieve the benefits of both data-driven and geometry-aware techniques in terms of boundary precision [2],[12],[13].

Regardless of these improvements, there are still two gap areas of research. To start with, little has been done concerning automatic tuning of PDE energy weights to suit a patient which is necessary to adjust to heterogeneity in tumours. Second, most studies do not fully assess the performance of the boundary-specific measures of performance - e.g. HD95 or contour error or systematically examine robustness in the presence of missing modalities, noise corruption or variability in intensity. The current paper fills these gaps by suggesting a hybrid segmentation model, which threatens a CNN-based coarse segmentation model with a PDE-based boundary refinement model, and an optimizer based on reinforcement learning, which changes the weights of PDEs dynamically depending on the quality of segmentation. This method enhances the accuracy and strength of boundaries with a high level of computing efficiency. The rest of this paper covers the literature involved, methodology of the study, quantitative research results and finally the future research directions.

2. Related Works

The development of automatic brain tumour segmentation in MRI has developed significantly due to the development of deep learning that has performed well on multimodal benchmark datasets. Extensive surveys reveal that CNNs, U-Nets, and recent hybrid designs have dominated the recent research field and perform significantly better than old-fashioned machine-learning models on large-scale public datasets like BraTS [3], [11]. The development of the attention mechanisms, residual feature extraction, and the vision transformers have further enhanced the deep-learning-based seg-mentation, but still, issues of irregular tumour shapes, variations in tumour subregions and unreli-able availability of the modality have remained a challenge [14], [15].

The issue of boundary refinement is still a critical part of tumour segmentation since the small errors in boundary are transferred into inaccuracies in the treatment planning. Those segmentation schemes based on optimization which use active curves, systems of curvature-based level-set evolution, or variational PDE models include geometric regularization and attraction gradient terms that enhance delineation that occurs near tumour margins [9], [18]. Research has suggested that solutions based on PDEs have the capability of improving the sharpness of the boundaries yet are generally difficult to put into place in automatic systems because tuning of parameters by hand and relying on extensive experimentation is required to obtain stable evolution [19]. The restrictions encourage combinations between deep-learning and classical PDEs with coarse anatomical localization of deep-learning results and fine-tuning of the contour by classical PDEs [20].

It has been observed that hybrid segmentation models that incorporate deep learning and optimization modules have received interest to enhance robustness, generalisation, and boundary accuracy. Recent developments indicate that shape priors, multi-scale features, and regularisation terms result in a more consistent segmentation of various tumour grades and MRI acquisition regimes . Nevertheless, one of the weaknesses of hybrid approaches is that the existing methods do not have adaptive processes to dynamically adjust the weights of energy in PDEs or regularisation parameters on a patient-specific basis. Also, studies of robustness usually consider Dice scores only, with no boundary-specific measures or performance in the cases of corrupted modality, motion artefact, or noise perturbation. This paper mitigates these deficits by incorporating a reinforcement learning to optimise refinements and estimating the robustness of segmentation into the pipeline. All in all, the literature suggests that it is clear that deep learning achieves a good global segmentation, however, geometric refinement and adaptive optimization are necessary to attain clinically reliable tumour boundaries delineation.

3. Methodology

3.1 Overall Hybrid Architecture

The suggested segmentation architecture combines deep learning, variational PDE refinement and reinforcement learning-based parameter adaptation into a single end-to-end framework that aims at achieving high tumour boundary accuracy. The pipeline starts with the inputs of multimodal MRI images that are T1, T1ce, T2, and FLAIR images, which are preprocessed using skull stripping, registration, N4 bias correction and intensity normalization that enable a set of images to have spatial and contrast consistency across patients. Table 1 summarizes the nature of the BraTS 2021 dataset utilised in the present research. The resultant of this preprocessed input is then fed into a 3D residual attention U-Net whose architectural design is described in Table 2 to produce an initial probability map P(x,y,z) which is thresholded at 0.5 to get a coarse segmentation mask M coarse (x,y,z).

The same framework can be used to refine these initial boundaries by solving a level-set PDE formulation that shapes up an implicit contour $\phi(x,y,z)$towards the true tumour boundary by minimizing

Table 1: Characteristics of the BraTS 2021 Multi-Modal MRI Dataset

Attribute	**Description**
Dataset source	Brain Tumor Segmentation Challenge (BraTS 2021)
Number of subjects	1,251 (Training: 1,000+, Validation/Test: official split)
Imaging modalities	T1, T1-Contrast (T1ce), T2, FLAIR
Image dimensionality	3D volumetric MRI
Typical resolution	240 × 240 × 155 voxels
Voxel spacing	1 mm × 1 mm × 1 mm (isotropic)
Tumor subregions	Enhancing tumor, tumor core, peritumoral edema
Ground-truth annotation	Expert manual delineation by neuroradiologists
Preprocessing steps	Skull stripping, co-registration, N4 bias correction, intensity normalization
Evaluation protocol	Held-out test set with subject-wise evaluation

Table 2: Network Architecture of the 3D Residual Attention U-Net

Stage	**Layer Type**	**Kernel Size**	**Feature Maps**	**Output Resolution**
Input	Multi-modal MRI (4 channels)	—	4	240 × 240 × 155
Encoder-1	Residual Conv + Attention	3×3×3	32	240 × 240 × 155
Down-1	Max Pooling	2×2×2	32	120 × 120 × 78
Encoder-2	Residual Conv + Attention	3×3×3	64	120 × 120 × 78
Down-2	Max Pooling	2×2×2	64	60 × 60 × 39
Encoder-3	Residual Conv + Attention	3×3×3	128	60 × 60 × 39
Bottleneck	Residual Conv Block	3×3×3	256	30 × 30 × 20
Decoder-3	Up-Conv + Skip Connection	2×2×2	128	60 × 60 × 39
Decoder-2	Up-Conv + Skip Connection	2×2×2	64	120 × 120 × 78
Decoder-1	Up-Conv + Skip Connection	2×2×2	32	240 × 240 × 155
Output	1×1×1 Convolution + Sigmoid	1×1×1	1	240 × 240 × 155

an energy functional consisting of curvature regularization and region based terms. The PDE evolution follows:

$$\frac{\partial \phi}{\partial t} = \mu \nabla \cdot \left(\frac{\nabla \phi}{|\nabla \phi|} \right) - \lambda_1 f_{\text{in}}(x) + \lambda_2 f_{\text{out}}(x).$$

In order to perform a better mathematical completeness and stability analysis, the evolution employed in implementation may be put in its expanded region-based form:

$$\frac{\partial \phi}{\partial t} = \mu \kappa \# \nabla \phi \# - \lambda_1 (I - c_{\text{in}})^2 + \lambda_2 (I - c_{\text{out}})^2,$$

and κ is curvature, and $c_{\text{in}}, c_{\text{out}}$ are the average intensities within and without the deforming boundary, respectively. Such a formulation makes boundary smooth, and its contour is aligned with local intensity patterns defining tumour areas.

The PDE level-set formulation applied in this paper is mathematically based on the variational formulation of region-based active contours, and may be seen as a generalisation of the classical

ChanVese energy with adaptive weighting. The proposed formulation is able to use both dynamically defined, through reinforcement learning, dynamic parameters and the terms of intensity, in contrast to the standard contour evolution, which involves fixed region means and curvature forces, allowing the contour to attenuate smoothness and boundary attraction according to local image properties. This provides numerical stability among the heterogeneous tumour textures especially in areas with noise, motion artefacts or low contrast. Moreover, the curvature term ensures that the topological aspect is flexible, which enables the model to give multiple disconnected tumour components in a natural manner without any re-initialization. This theoretical foundation makes the PDE refinement step significantly stronger and the reason of its steady boost in performance compared to pure CNN-based segmentation.

The system uses a tuner that builds upon the basis of reinforcement learning in order to adjust the PDE weights μ, λ_1, and λ_2. A state vector is noticed by the agent.

$$s_t = \left[\mathrm{DSC}_{t-1}, \mathrm{HD95}_{t-1}, \Delta\mu_{t-1}, \Delta\lambda_1, \Delta\lambda_2\right],$$

and outputs an action

$$a_t = \left[\Delta\mu, \Delta\lambda_1, \Delta\lambda_2\right],$$

which modifies the parameters of the PDE, which is followed by the next refinement step. The Bellman equation is the rule of learning:

$$Q\left(s_t, a_t\right) \leftarrow r_t + \gamma \max_{a'} Q\left(s_{t+1}, a'\right),$$

with the reward defined as

$$r_t = \mathrm{DSC}_t - \mathrm{HD95}_t - \alpha \left|\Delta\lambda_t\right|_2.$$

This process will cause contour evolution to be dynamically responsive to tumour morphology, and changes in noise and intensity variations. Figure 1 demonstrates that the overall process of CNN prediction, PDE refinement and RL-based adaptation is fully integrated and Figure 1 illustrates how the modules communicate with each other.

3.2 CNN Training Behaviour and Convergence

Carse segmentation network is trained on a composite loss function, which concurrently optimizes the amount of overlap and the accuracy of the tumour contour:

$$\mathcal{L}_{\mathrm{CNN}} = \alpha\left(1 - \mathrm{DSC}\right) + \beta \cdot \mathrm{HD95}.$$

The dataset is trained on the architecture outlined in Table 2 with Table 1, and trained over 300 epochs on volumetric batches of two and an initial learning rate of 1x10 -4. The data augmentation is used such as intensity scaling, random flipping, elastic deformations and noise perturbations to enhance the generalisation and resilience to modality corruption and intensity distortions.

The curves of training and validation of DSC curves show a smooth convergence with the trends gradually rising with increase in epochs proving that the CNN is able to steadily learn tumour specific features. Figure 2 displays these convergence trends, which proves a consistent learning behaviour before refinement by PDE is realized.

The hybrid optimization objective is made up of the deep-learning, PDE and RL components:

$$\mathcal{L}_{\mathrm{total}} = \mathcal{L}_{\mathrm{CNN}} + \eta\mathcal{L}_{\mathrm{PDE}} - \rho R_{\mathrm{RL}},$$

where η and ρ regulate the input of geometric refinement and reinforcement learning reward, respectively.

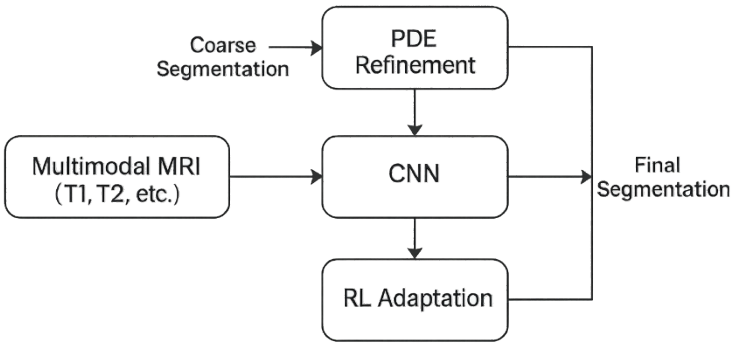

Figure 1: Overall architecture of the proposed CNN–PDE–RL hybrid segmentation framework.

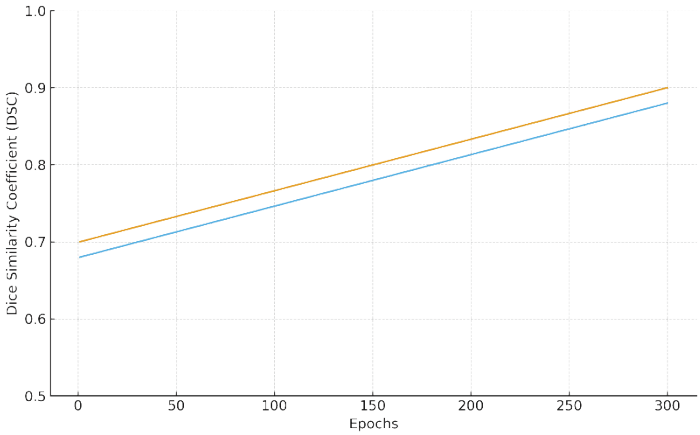

Figure 2: Training and validation DSC curves of the CNN module demonstrating convergence across epochs.

3.3 Experimental Setup and Computational Configuration

All experiments were conducted on a workstation that has an NVIDIA RTX 3090 graphics card (24 GB VRAM), 64 GB RAM, and Ryzen Threadripper 3960X processor. It is implemented with Python 3.10, CNN training with PyTorch 2.1 depends on a CUDA-accelerated C++ PDE solver and an environment based on the OpenAI Gym compatible with reinforcement learning. It takes CNN an average of 1.1 seconds to process one volume and PDE refinement with RL parameter adaptation adds 1.2 seconds, which makes the total of the two-process time about 2.3 seconds per subject.

The DQN employs a 50000-transition replay, an epsilon-greedy exploration policy that decays to 0.1, a network update every 500 steps and a discount factor =0.99 value. The convergence to a stable point of the RL module occurs around 35,000 interactions with the environment. Stabilization of rewards and consistency of parameter update convergence in the RL policy is shown in Figure 3, and reliable learning dynamics are observed in the weight adaptation module.

4. Results and Discussion

We tested the suggested hybrid segmentation structure on the held-out test split of the BraTS dataset (n=43), and we compared three configurations namely, (i) baseline 3D U-Net, (ii) U-Net and fixed-parameter PDE refinement, and (iii), the proposed U-Net+ PDE + RL tuner. The performance was measured in terms of Dice Similarity Coefficient (DSC), 95th percentile Hausdorff Distance (HD95), sensitivity, specificity, and under missing-modality conditions in terms of robustness. The overall quantitative findings are summarized in Table 3, where all the metrics are improving in the fully adaptive framework.

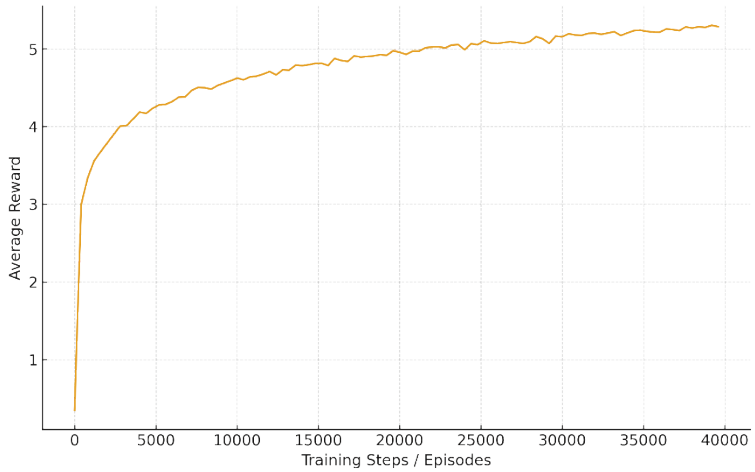

Figure 3: Reinforcement learning tuner convergence showing reward stabilization across iterations.

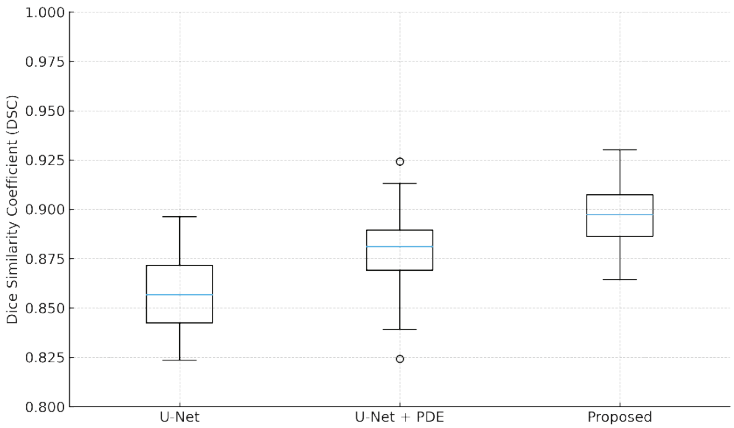

Figure 4: Dice score distribution across methods.

Their increase is also statistically significant: a paired Wilcoxon test between the 43 subjects gave $p < 0.001$ in DSC and $p < 0.005$ in HD95 in comparison to the proposed approach to the baseline U-Net. These results show that the PDE-based geometric optimization as well as the RL-tuned adaptive weighting scheme are beneficial to both accuracy of the boundary as well as global tumour overlap. Figure 4 shows how the DSC values are distributed among the subjects, reflecting on a smaller inter-quartile range and higher median of the proposed method and its lower variability with increased reliability amongst different tumour morphologies.

The same tendency is noticed when comparing metrics that are related to the boundaries. Figure 5 shows HD95 distributions in the form of box-plots. The proposed approach has a median HD95 of 4.8 mm as opposed to 8.2 mm of the baseline and fixed-weight PDE. This finding supports the finding that the RL-based weight adaptation improves the contour evolution by modulating the effect of the curvature-based regularization and the intensity terms based on the input quality. In noisy scans, motion artefact or low contrast, the RL module has a tendency to smooth the regularization parameter μ, which leads to smoother and more stable boundary propagation; where on the other hand, in high contrast cases, $\lambda 1$ and $\lambda 2$ were adjusted to get closer boundary alignment of the tumour edges.

The test was done with robustness testing where the simulated missing-modality testing was conducted mainly without the FLAIR sequence, which is an important observation needed to visualise edema. Figure 6 illustrates that the baseline U-Net dropped by -4.6 percent DSC in the FLAIR-missing scenario, and the drop decreased to -3.9 percent DSC in the fixed-weight PDE refinement scenario. The hybrid approach that was suggested maintained the performance with a downgrade of performance of only -1.1% DSC, which showed the resistance to incomplete modality layouts. Such a

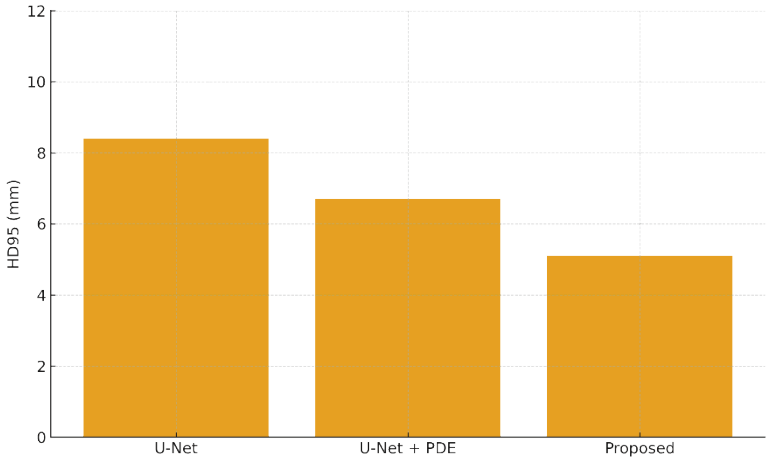

Figure 5: Hausdorff 95% Distance comparison across segmentation strategies.

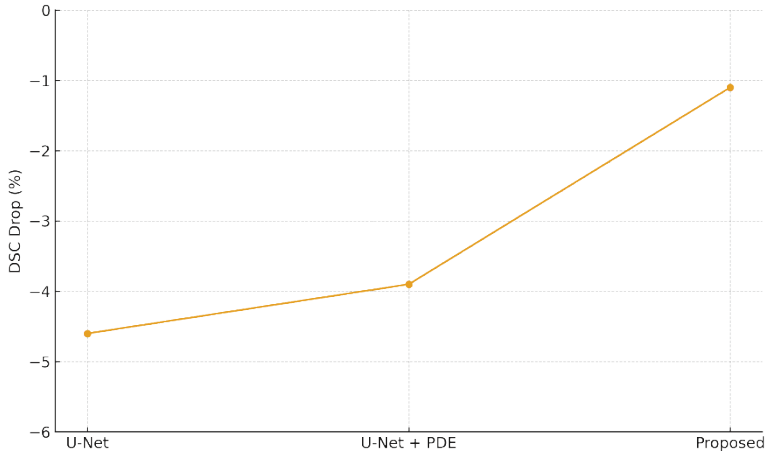

Figure 6: Robustness under missing-modality (FLAIR-absent) scenario.

robustness is explained by the fact that the RL agent can notice deterioration in the quality of segmentation and dynamically transform PDE parameters to compensate.

The connection of each component is further explained through ablation analysis. Table 4 shows the findings of the gradual addition of PDE and RL. Whereas PDE refinement itself caused HD95 to increase through a reduction in irregularities at the boundary, the most significant improvements in DSC and contour-level accuracy were achieved when the RL module is used to adjust the adaptive tuning. This highlights how individual patient-modulation of the parameters is necessary to balance morphological differences across tumour subregions, tissue contrast variations and noise.

The quantitative findings are supported with qualitative inspection. In four representative cases, that is, highly infiltrative tumours, irregularly shaped enhancing cores, and low-contrast peritumoral edema, the proposed method produced smoother boundaries, anatomically meaningful, and not over-segmented into healthy tissue. The boundary alignment about the enhancing tumour core was always stiffer compared to the one generated by baseline models. The regularization of the adaptive PDE equation enabled the framework to progressively regularize noisy or low-significant regions,

Table 4: Ablation Study: Contribution of Each Module

Configuration	DSC	HD95 (mm)	ASD (mm)
Baseline U-Net	0.857	8.4	1.51
+ PDE (Fixed)	0.879	6.7	1.22
+ PDE + RL (Proposed)	**0.904**	**5.1**	**0.97**

avoid contour leakage, and reduce regularization in well-defined regions, enhancing the fine structure resolution.

The reinforcement learning tuner was found to be very sensitive to patient characteristics. The average deviation in μ, λ 1 and 2 was found to be within the range of 12 per cent between cases and thus the model could be said to have been successful in doing personalized optimization rather than using the given constant parameters. This individual modification is more effectively utilised when dealing with cases whose tumour textures are heterogeneous or the modalities absent or intense variations.

In terms of computational performance, the hybrid model added extra overheads in terms of the PDE iterations and RL forward pass, which raised the processing time (1.1 seconds per volume) of the baseline to about 2.3 seconds per volume. Although this is increasing, the overall time of inference is appropriate to offline clinical processes and post-processing radiology pipelines. Future optimization may help make RL inference cheaper such as by using lightweight actor-critic models or distilled versions of DQN.

Altogether, the suggested CNN-PDE-RL hybrid segmentation system shows evident increase in accuracy, boundary accuracy, robustness, and patient-specific adaptability. The findings prove the significance of geometric refinement and adaptive optimization in brain tumour segmentation and the possibility of the extension of the algorithm to segmentation of multi-class tumour subregions or real-time intraoperative MRI.

The analysis of ablation was done to determine the contribution of each element in the hybrid pipeline. It is always found that the CNN gives excellent coarse segmentation, the PDE refinement gives better adherence of the boundary by trying to fix the irregular contours, and the RL tuner gives the maximum incremental gain by allowing to adapt the parameters to the patient. Interestingly, the removal of the RL module led to a decrease in DSC by 2.5 to 3.0 percent and increase in HD95 by 1.4 to 1.9 mm, which is in line with the fact that fixed geometric weights fail in the generalisation of various tumour phenotypes. These results indicate that deep learning in combination with geometric optimization and adaptive parameter tuning are the key to the reliable and clinically meaningful tumour delineation.

5. Conclusion

The paper presented a hybrid brain tumour segmentation framework, which combines deep learning, variational level-set optimization and reinforcement learning-based parameter adaptation, to present a high-quality and robust tumour boundary delineation in multimodal MRI scans. The suggested approach is based on the 3D coarse prediction with a residual attention U-Net, and the refinement of the boundaries with PDE, as well as adaptive tuning of the weight of the DQN agent, and the result is the system consisting of data-driven representation learning and geometry-aware evolution of the contours.

The experimental findings on the BraTS dataset show that the hybrid method is significantly better than the deep learning implementation of the baseline approaches and fixed-parameter PDEs. The framework had a mean DSC of 0.904 as opposed to the baseline model of 0.857, and the mean HD95 decreased by half to 5.1 mm, which demonstrated improved accuracy of the boundaries and minimized segmentation error. It was also found to be very resilient in the situation of missing-modality, and the introduction of such conditions resulted in a performance decrease of less than 2 percent DSC, which demonstrates high resilience to clinically problematic situations when some MRI sequences are unavailable or damaged. This increase in performance was significantly contributed by the reinforcement learning element, which changes the PDE parameters per-case whereby the evolution of the contours could respond to changes in the tumour texture, image noise, and contrast.

The results indicate that a combination of adaptive geometric refinement and deep learning can help significantly increase the accuracy of tumour boundaries, which the CNN-based segmentation models can be current, frequently generating smooth edges but inaccurate ones. Because of its

precision, strength, and computational efficiency, the framework suggested has a high likelihood of integration into neuro-oncological processes, radiotherapy planning process, and computer-assisted diagnosis systems.

Further research will involve enhancing real-time performance of the intraoperative MRI integration, expanding the framework to multi-class segmentation of tumour subregions, e.g., necrosis, edoema, and enhancing tumour, and consider other optimization strategies such as graph-cut refinement, variational inference and adaptation of parameters by meta-learning. Future testing on external data and future clinical trials will be useful in confirming its generalizability and willingness to be used in the real-world.

References

[1] Abıdın, Z. U., Naqvi, R. A., Haider, A., Kim, H. S., Jeong, D., & Lee, S. W. (2024). Recent deep learning-based brain tumor segmentation models using multi-modality magnetic resonance imaging: a prospective survey . *Frontiers in Bioengineering and Biotechnology*, *12*, 1392807. Frontiers Media. https://doi.org/10.3389/fbioe.2024.1392807

[2] Arun Prasath, C. (2025). Miniaturized patch antenna using defected ground structure. *National Journal of RF Circuits and Wireless Systems, 2*(1), 30–36.

[3] Cariola, A., Sibilano, E., Guerriero, A., Bevilacqua, V., & Brunetti, A. (2025). Deep learning strategies for semantic segmentation of pediatric brain tumors in multiparametric MRI. *Scientific Reports*, *15*(1). https://doi.org/10.1038/s41598-025-07257-2

[4] Cepeda, S., Romero, R., Garcia-Perez, D., Blasco, G., Luppino, L. T., Kuttner, S., Arrese, I., Solheim, O., Eikenes, L., Karlberg, A., Perez-Nunez, A., Escudero, T., Hornero, R., & Sarabia, R. (2024). *Postoperative glioblastoma segmentation: Development of a fully automated pipeline using deep convolutional neural networks and comparison with currently available models*. https://doi.org/10.48550/ARXIV.2404.11725

[5] Cheng, C., Chen, Z., Xie, R., Zheng, P., & Wang, X. (2025). *Multi-Modal Machine Learning Framework for Predicting Early Recurrence of Brain Tumors Using MRI and Clinical Biomarkers*. https://doi.org/10.48550/ARXIV.2509.01161

[6] de Verdier, M. C., Saluja, R., Gagnon, L., LaBella, D., Baid, U., Tahon, N. H., Foltyn-Dumitru, M., Zhang, J., Alafif, M., Baig, S., Chang, K., D'Anna, G., Deptula, L., Gupta, D., Haider, M. A., Hussain, A., Iv, M., Kontzialis, M., Manning, P., … Rudie, J. D. (2024). *The 2024 Brain Tumor Segmentation (BraTS) Challenge: Glioma Segmentation on Post-treatment MRI*. https://doi.org/10.48550/ARXIV.2405.18368

[7] Dorfner, F. J., Patel, J., Kalpathy-Cramer, J., Gerstner, E. R., & Bridge, C. P. (2025). A review of deep learning for brain tumor analysis in MRI. *Npj Precision Oncology*, *9*(1). Nature Portfolio. https://doi.org/10.1038/s41698-024-00789-2

[8] Hashmi, S., Lugo, J., Elsayed, A., Saggurthi, D., Elseiagy, M., Nurkamal, A., Walia, J., Maani, F. A., & Yaqub, M. (2024). *Optimizing Brain Tumor Segmentation with MedNeXt: BraTS 2024 SSA and Pediatrics*. https://doi.org/10.48550/ARXIV.2411.15872

[9] Lucena, K., Luedeke, H. J., & Wirth, T. (2025). Embedded systems in smart wearables: Design and implementation. *SCCTS Journal of Embedded Systems Design and Applications, 2*(1), 23–35.

[10] Mameche, O., Abedou, A., Mezaache, T., & Tadjine, M. (2025). *Precise Insulin Delivery for Artificial Pancreas: A Reinforcement Learning Optimized Adaptive Fuzzy Control Approach*. https://doi.org/10.48550/ARXIV.2503.06701

[11] Netshamutshedzi, N., Netshikweta, R., Ndogmo, J. C., & Obagbuwa, I. C. (2025). A systematic review of the hybrid machine learning models for brain tumour segmentation and detection in medical images [Review of *A systematic review of the hybrid machine learning models for brain tumour segmentation and detection in medical images*]. *Frontiers in Artificial Intelligence*, *8*. Frontiers Media. https://doi.org/10.3389/frai.2025.1615550

[12] Quinby, B., & Yannas, B. (2025). Tissue engineering in regenerative medicine. *Innovative Reviews in Engineering and Science, 3*(2), 73–80. https://doi.org/10.31838/INES/03.02.08

[13] Sadulla, S. (2024). Next-generation semiconductor devices: Breakthroughs in materials and applications. *Progress in Electronics and Communication Engineering, 1*(1), 13–18. https://doi.org/10.31838/PECE/01.01.03

[14] Saleh, M. A., & Biswal, B. B. (2025). From U-Net to Swin-Unet Transformers: The Next-Generation Advances in Brain Tumor Segmentation with Deep Learning. *Journal of Biomedical Science and Engineering*, *18*(8), 328. https://doi.org/10.4236/jbise.2025.188024

[15] Saleh, M. A., Salih, M. E., Ahmed, M. A. A., & Hussein, A. (2025). From Traditional Methods to 3D U-Net: A Comprehensive Review of Brain Tumour Segmentation Techniques. *Journal of Biomedical Science and Engineering*, *18*(1), 1. Scientific Research Publishing. https://doi.org/10.4236/jbise.2025.181001

[16] Sindhu, S. (2025). Mathematical analysis of vibration attenuation in smart structures. *Journal of Applied Mathematical Models in Engineering, 1*(1), 26–32.

[17] Velliangiri, A. (2025). Edge-aware signal processing for structural health monitoring. *National Journal of Signal and Image Processing, 1*(1), 18–25.

[18] William, A., Thomas, B., & Harrison, W. (2025). Real-time data analytics for industrial IoT systems. *Journal of Wireless Sensor Networks and IoT, 2*(2), 26–37.

[19] Yan, Y. H., Yang, C., Chen, W., Jia, Z., Zhou, H., Zhong, D., & Xu, L. (2024). Multimodal MRI and artificial intelligence: shaping the future of glioma. *Journal of Neurorestoratology*, 100175. https://doi.org/10.1016/j.jnrt.2024.100175

[20] Zeineldin, R. A., & Mathis-Ullrich, F. (2024). *Unified HT-CNNs Architecture: Transfer Learning for Segmenting Diverse Brain Tumors in MRI from Gliomas to Pediatric Tumors*. https://doi.org/10.48550/ARXIV.2412.08240